In the Spotlight: Biomedical Imaging

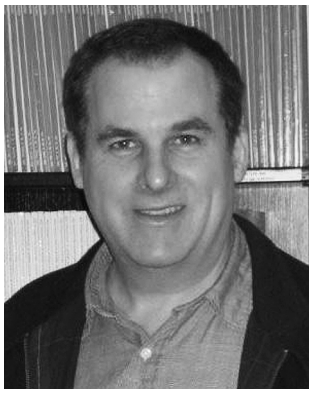

Andrew F. Laine, *Senior Member, IEEE*

I. Introduction

BIOMEDICAL imaging plays a critical role for the life sciences and health care. In the previous year, we had given a broad snapshot of biomedical imaging advances ranging from applications in systems biology to clinical applications in health care involving computer-aided diagnosis (CAD) and integrated picture archiving systems (PACS) [1].

This spotlight resumes on a selected set of topics and collects promising and recent research advances in the field of multi-modal temporal data analysis [2], [3], [4], high-field magnetic resonance spectroscopy [5]–[10], trends in computer-aided diagnosis [11]–[15] and advances in cardiac diagnostic imaging. In the first section we briefly point to promising work on statistical models for tracking, detection, and segmentation in multi-modal temporal imagery. Section III will give a brief snapshot of slice selective free induction decay (FID) acquisition for 7 Tesla high-field MR imaging. Section IV will outline highlights in comparative validation of computer-aided diagnosis and associated image analysis algorithms spanning a variety of application domains from the heart to the eye [11], [12], [15]. Lastly, Section V describes advances in the analysis of real-time three-dimensional (3-D) echocardiography for computing myocardial strain.

II. Multi-Modal Temporal Data Analysis

Technical advances in multi-modal imaging provide us with longitudinal multi-modal imagery that is often unexplored in its richness of information during the diagnostic decision process. Emerging applications are multiple-sclerosis lesion tracking, detection of edema progression [3], and temporal tumor segmentation [2].

In [3] the authors presented research on edema detection in longitudinal multi-modal brain magnetic resonance images with minimal expert intervention. By combining transductive and inductive machine learning methods the approach allowed to automatically extract regions of phenotypic disorders. The study also investigated optimal sets of minimal annotations that are required per single time point and across time to perform longitudinal detection of edema regions. Empirical validation of optimal feature sets and multi-modality features showed that feature combinations from multi modalities lead to increased detection performance compared to single modality features with an 88.6% true positive rate. This technology can have a tremendous impact and significance on identifying cost effective clinical decisions for patient specific outcome. In addition, advances in longitudinal data analysis can provide the infrastructure to support comparative studies in systemic diseases such as arterial sclerosis.

III. High-Field MR Spectroscopy

While MR spectroscopy has been studied for well over 20 years, its broad clinical use has been difficult and limited due to frequency specific interactions that need to be taken into account for each protocol and study. However, this year we began to see the emergence of protocols that that may lead to commercial application of MR spectroscopy in both 3 T and 7 T systems [10]. For example, metabolite levels in the brain have been shown to be linked to several pathologies such as multiple sclerosis (MS) [8], Alzheimer's [5] and even depression [6]. The accurate measurement of the metabolic levels is therefore crucial for a proper diagnosis. Magnetic resonance spectroscopy is the tool of choice for this purpose. Current 3 T scanners allow the quantification of only 6 metabolites: N-acetyl-aspartate (NAA), choline, creatine, myo-inositol (ml), lactate (Lac) and the sum of glutamate (Glu) and glutamine (Gln) [10]. On the other hand, at

Manuscript received September 28, 2009; revised September 28, 2009. Current version published November 18, 2009.
A. F. Laine is with the Department of Biomedical Engineering, Columbia University, New York, NY 10027 USA (e-mail: laine@columbia.edu).
Digital Object Identifier 10.1109/RBME.2009.2034700

higher fields (7 T) there is an increase in signal-to-noise (SNR) and up to 18 metabolites can be quantified. These gains come at a price, however. As the strength of the magnetic field increases, the T2 relaxation times get shorter due to increased effects of susceptibility differences [7], [9]. This implies that any SNR gain is lost due to relaxation effects and that shorter and shorter echoes are needed in order to capture the metabolite signal. Although sequences exist that have ultra short echo times, those typically suffer from severe limitations on the maximum achievable B1 field strength. This is due in part to patient safety and FDA mandated SAR guidelines. As a result, the bandwidth available for the amplitude-modulated RF pulses is significantly decreased. A further issue that is exacerbated at ultrahigh fields is the large chemical shift displacement artifact. Although it is possible to overcome this problem using frequency-modulated RF pulses, those typically require long durations to achieve the desired effect. The minimal echo time becomes excessive then, causing severe T2 losses.

To overcome these contradictory problems, one possible method is the acquisition of the free induction decay (FID) [10], thus eliminating the need for an echo time. A frequency-modulated excitation pulse is used for slice-selection and to minimize the chemical shift displacement artifact. In plane localization is achieved using an outer-volume-suppression (OVS) scheme which also reduces the signal from skull lipids. Given the large B1 variations in the head-feet direction at 7 T, OVS cannot be used for 3-D localization. The VAPOR sequence is used for water suppression and is interleaved with the OVS. The new protocol allows for the quantification and mapping of 12 metabolites, a significant improvement over the six classically detected using lower field magnets.

IV. Computer-Aided Diagnosis (CAD)

In recent years, several application domains reported on standardized image databases and comparative assessment of computer-aided diagnosis and their associated image analysis algorithms.

In the field of lung cancer screening ImageCLEF [14], ANODE09 [13], and the public lung database (PLB) [16] are recent initiatives that provide means for comparative assessment of pulmonary nodule detection with standardized unified validation metrics. Other recent comparative CAD assessments include the Rotterdam coronary artery evaluation framework [11] and the segmentation challenge of prostate, head, neck, and the heart [17]. The trend of standardized image databases and comparative CAD assessment research for combining CAD algorithms show great promise to improve on state of the art performance of single CAD schemes.

In [15] the authors address a question on optimal information fusion of multiple CAD algorithms for the automatic detection of normal and abnormal diabetic retinopathy cases. Several different fusion methods were proposed and their effect on the performance of a complete comprehensive automatic diabetic retinopathy screening system was evaluated. The complete system was evaluated on a set of 15 000 exams (60 000 images). The best performing fusion method obtained an area under the receiver operator characteristic curve (AUC) of 0.881.

V. 4-D Ultrasound Imaging

Real-time 3-D imaging or four-dimensional (4-D) ultrasound remains an exciting application as it expands the field of view from a two-dimensional (2-D) slice to full 3-D volumes in time. Real-time 3-D echocardiography offers an efficient way to capture complex 3-D dynamic motion of the heart. Over the past five years, commercial 4-D ultrasound systems have been developed by Philips Medical Systems (Andover, MA) in the SONOS 7500, followed by the iE33 model, GE Vivid 7 and E9, Siemens SC2000 and Toshiba Artida [18]. Dynamic cardiac metrics, including myocardial strain and displacement, can provide a quantitative approach to evaluate cardiac function [18]–[23], wall motion and ischemia. The complex 3-D wall motion and temporal information contained in these 4-D data sequences have the potential to enhance and supplement other imaging modalities for clinical diagnoses including cardio-rehabilitative therapy (CRT) for placement of pacemaker lead optimization. However, in current commercial clinical diagnostic [19], [24] systems, only 2-D strain measures are used despite that cardiac motion is complex and inherently 4-D in nature. Recent advances in the analysis of 4-D cardiac ultrasound include an optical flow based method developed to estimate full 4-D dynamic cardiac metrics, including strains and displacements in real time from streaming 4-D ultrasound [18]. Such methods of analysis can provide a clinically effective 3-D strain-and-torsion measuring tool that will allow cardiologists to routinely characterize cardiac wall motion and strain with reliable accuracy. Thus, the realization of real time computation of 3-D strain of the myocardium will permit physicians to localize infarcted or ischemic tissue that can be salvaged by intervention and recognize at an early stage.

Acknowledgment

Andrew F. Laine would like to express his appreciation to Noah Lee, Ouri Cohen, and Auranuch Lorsakul for their efforts and the outstanding contributions.

References

[1] A. F. Laine, "In the spotlight: Biomedical imaging," *IEEE Rev. Biomed. Eng.*, vol. 1, pp. 4–7, 2008.

[2] T. Riklin Raviv, B. H. Menze, K. Van-Leemput, B. Stieltjes, M. A. Weber, N. Ayache, W. M. Wells, III, and P. Gollland, "Joint segmentation via patient-specific latent anatomy model," in *Proc. MICCAI Workshop on Probabilistic Methods for Medical Image Analysis*, London, U.K., 2009.

[3] J. J. Caban, N. Lee, S. Ebadollahi, A. Laine, and R. DeLaPaz, "Concept detection in longitudinal brain MR images using multi-modal cues," in *Proc. 6th IEEE Int. Symp. Biomedical Imaging (ISBI): From Nano to Macro*, Boston, MA, 2009.

[4] N. Lee, J. Caban, S. Ebadollahi, and A. F. Laine, "Interactive segmentation in multi-modal medical imagery using a bayesian transductive learning approach," in *Proc. SPIE Medical Imaging*, FL, USA, 2009, vol. 7260, pp. 72601W–72601W10 , , , and , "," , vol. , pp. –, .

[5] T. K. Shonk, R. A. Moats, P. Gifford, T. Michaelis, J. C. Mandigo, J. Izumi, and B. D. Ross, "Probable Alzheimer disease: Diagnosis with proton MR spectroscopy," *Radiol.*, vol. 195, pp. 65–72, 1995.

[6] A. Kumar, A. Thomas, H. Lavretsky, K. Yue, A. Huda, J. Curran, T. Venkatraman, L. Estanol, J. Mintz, M. Mega, and A. Toga, "Frontal white matter biochemical abnormalities in late-life major depression detected with proton magnetic resonance spectroscopy," *Amer. J. Psychiatry*, vol. 159, pp. 630–636, 2002.

[7] I. Tkac, P. Andersen, G. Adriany, H. Merkle, K. Ugurbil, and R. Gruetter, "*In vivo* H1 NMR spectroscopy of the human brain at 7 T," *Magnetic Resonance Imaging*, vol. 46, pp. 451–456, 2001.

[8] O. Gonen, D. M. Moriarty, B. S. Y. Li, J. S. Babb, J. He, J. Listerud, D. Jacobs, C. E. Markowitz, and R. I. Grossman, "Relapsing-remitting multiple sclerosis and whole-brain N-acetylaspartate measurement: Evidence for different clinical cohorts-initial observations," *Radiol.*, vol. 225, pp. 261–268, 2002.

[9] R. Otazo, B. Mueller, K. Ugurbil, L. Wald, and S. Posse, "Signal-to-noise ratio and spectral linewidth improvements between 1.5 and 7 Tesla in proton echo-planar spectroscopic imaging," *Magnetic Resonance Imaging*, vol. 56, pp. 1200–1210, 2006.

[10] A. Henning, A. Fuchs, J. B. Murdoch, and P. Boesiger, "Slice selective FID acquisition, localized by outer volume suppression (FIDLOVS) for (1)H-MRSI of the human brain at 7 T with minimal signal loss," *NMR Biomed.*, vol. 22, pp. 683–696, 2009.

[11] M. Schaap, C. T. Metz, T. v. Walsum, A. G. v. d. Giessen, A. C. Weustink, N. R. Mollet, C. Bauer, H. Bogunović, C. Castro, X. Deng, E. Dikici, T. O'Donnell, M. Frenay, O. Friman, M. H. Hoyos, P. H. Kitslaar, K. Krissian, C. Kühnel, M. A. Luengo-Oroz, M. Orkisz, Ö. Smedby, M. Styner, A. Szymczak, H. Tek, C. Wang, S. K. Warfield, S. Zambal, Y. Zhang, G. P. Krestin, and W. J. Niessen, "Standardized evaluation methodology and reference database for evaluating coronary artery centerline extraction algorithms," *Med. Image Anal.*, vol. 13, pp. 701–714, 2009.

[12] K. Murphy, B. van Ginneken, A. M. R. Schilham, B. J. de Hoop, H. A. Gietema, and M. Prokop, "A large-scale evaluation of automatic pulmonary nodule detection in chest CT using local image features and k-nearest neighbour classiciation," *Med. Image Anal.*, vol. 13, pp. 757–770, 2009.

[13] B. van Ginneken, S. G. Armato, III, B. de Hoop, S. van de Vorst, T. Duindam, M. Niemeijer, K. Murphy, A. M. R. Schilham, A. Retico, M. E. Fantacci, N. Camarlinghi, F. Bagagli, I. Gori, T. Hara, H. Fujita, G. Gargano, R. Belloti, F. De Carlo, R. Megna, S. Tangaro, L. Bolanos, P. Cerello, S. C. Cheran, E. Lopez Torres, and M. Prokop, Comparing and combining algorithms for computer-aided detection of pulmonary nodules in computed tomography scans: The ANODE09 study 2009 [Online]. Available: http://anode09.isi.uu.nl/technicalreportanode.pdf.

[14] B. Caputo, T. Tommasi, H. Mueller, T. M. Deserno, and J. Kalpathy-Cramer, ImageCLEF lung nodule detection and medical annotation task 2009 [Online]. Available: http://www.imageclef.org/2009/medanno.

[15] M. Niemeijer, M. Abramoff, and B. v. Ginneken, "Information fusion for diabetic retinopathy CAD in digital color fundus," *IEEE Trans. Med. Imag.*, vol. 28, pp. 775–785, 2009.

[16] A. P. Reeves, A. M. Biancardi, D. Yankelevitz, S. Fotin, B. M. Keller, A. Jirapatnakul, and J. Lee, "A public image database to support research in computer aided diagnosis," in *Proc. 31st Annu. Int. Conf. IEEE EMBS*, Minneapolis, MN, 2009, pp. 3715–3718.

[17] W. Niessen, T. van Walsum, R. Hameeteman, L. Joskowicz, N. Hata, G. Fichtinger, V. Pekar, and P. Radau, 3D segmentation in the clinic: A grand challenge 2009 [Online]. Available: http://grand-challenge2009.bigr.nl.

[18] Q. Duan, E. D. Angelini, S. L. Herz, C. M. Ingrassia, K. D. Costa, J. W. Holmes, S. Homma, and A. F. Laine, "Region-based endocardium tracking on real-time three-dimensional ultrasound," *Ultrasound in Medicine and Biol.*, vol. 35, pp. 256–265, 2009.

[19] E. Angelini, S. Homma, G. Pearson, J. Holmes, and A. Laine, "Segmentation of real-time three-dimensional ultrasound for quantification of ventricular function: A clinical study on right and left ventricles," *Ultrasound in Medicine and Biol.*, vol. 31, pp. 1143–1158, 2005.

[20] J. Crosby, B. H. Amundsen, T. Hergum, E. W. Remme, S. Langeland, and H. Torp, "3-D speckle tracking for assessment of regional left ventricular function," *Ultrasound in Medicine and Biol.*, vol. 35, pp. 458–471, March 2009.

[21] X. Chen, H. Xie, R. Erkamp, K. Kim, C. Jia, J. Rubin, and M. O'Donnell, "3-D correlation-based speckle tracking," *Ultrasound Imaging*, pp. 21–36, 2005.

[22] A. Elen, H. F. Choi, D. Loeckx, H. Gao, P. Claus, P. Suetens, F. Maes, and J. D'hooge, "Three-dimensional cardiac strain estimation using spatio-temporal elastic registration of ultrasound images: A feasibility study," *IEEE Trans. Med. Imag.*, vol. 27, pp. 1580–1591, 2008.

[23] W. Yu, P. Yan, A. J. Sinusas, K. Thiele, and J. S. Duncan, "Towards pointwise motion tracking in echocardiographic image sequences: Comparing the reliability of different features for speckle tracking," *Med. Image Anal.*, vol. 10, pp. 495–508, 2006.

[24] M. Toshiyuki Hata, M. Shu-Yan Dai, M. Eisuke Inubashiri, M. Kenji Kanenishi, M. Hirokazu Tanaka, M. Toshihiro Yanagihara, and R. Seiko Araki, "Four-dimensional sonography with B-flow imaging and spatiotemporal image correlation for visualization of the fetal heart," *J. Clin. Ultrasound*, vol. 36, pp. 204–207, 2008.